

See discussions, stats, and author profiles for this publication at: <https://www.researchgate.net/publication/41147723>

Stopped-flow studies of the reaction of D-tartronate semialdehyde-2-phosphate with human neuronal enolase and yeast enolase 1

ARTICLE *in* FEBS LETTERS · MARCH 2010

Impact Factor: 3.17 · DOI: 10.1016/j.febslet.2010.01.042 · Source: PubMed

CITATIONS

2

READS

29

3 AUTHORS, INCLUDING:



[John M Brewer](#)

University of Georgia

96 PUBLICATIONS 1,949 CITATIONS

SEE PROFILE



[Robert Stephen Phillips](#)

University of Georgia

216 PUBLICATIONS 3,747 CITATIONS

SEE PROFILE



Stopped-flow studies of the reaction of D-tartronate semialdehyde-2-phosphate with human neuronal enolase and yeast enolase 1

John M. Brewer^{a,*}, Jared S. McKinnon^a, Robert S. Phillips^b

^a Department of Biochemistry and Molecular Biology, University of Georgia, Athens, GA 30602, United States

^b Department of Chemistry, University of Georgia, Athens, GA 30602, United States

ARTICLE INFO

Article history:

Received 4 December 2009

Revised 14 January 2010

Accepted 16 January 2010

Available online 26 January 2010

Edited by Miguel De la Rosa

Keywords:

Stopped-flow

Subunit interaction

Enolase

Enolase mechanism

ABSTRACT

We determined the kinetics of the reaction of human neuronal enolase and yeast enolase 1 with the slowly-reacting chromophoric substrate D-tartronate semialdehyde phosphate (TSP), each in tris (tris (hydroxymethyl) aminomethane) and another buffer at several Mg^{2+} concentrations, 50 or 100 μM , 1 mM and 30 mM. All data were biphasic, and could be satisfactorily fit, assuming either two successive first-order reactions or two independent first-order reactions. Higher Mg^{2+} concentrations reduce the relative magnitude of the slower reaction. The results are interpreted in terms of a catalytically significant interaction between the two subunits of these enzymes.

© 2010 Federation of European Biochemical Societies. Published by Elsevier B.V. All rights reserved.

1. Introduction

Enolase (E.C.4.2.1.11; 2-phospho-D-glycerate hydrolyase) catalyzes and hence controls the ninth reaction of glycolysis, so is ubiquitous in living organisms. The enzyme requires two moles of Mg^{2+} (the physiological cofactor) per active site [1]: “conformational” Mg^{2+} enables the physiological substrate (2-PGA, 2-phospho-D-glycerate), product (PEP, phosphoenolpyruvate) or analogues (such as the slowly-reacting strongly bound substrate D-tartronate semialdehyde phosphate (TSP)) to bind. This in turn enables “catalytic” Mg^{2+} to bind and produce catalysis [1,2].

Direct measurements of PEP production from 2-PGA are conventionally done at 230 nm [2,3]; TSP is thought to enolize when bound to enolases [4], and this reaction is often measured at 285 nm. Proton removal from carbon-2 is rate limiting with both reactions [5,6], at least at pH values near the optimum. Hence, the TSP reaction is thought to reflect the earliest stage(s) of the physiological reaction.

Enolases are generally abundantly expressed, so are major cellular proteins [7]. In addition, the enzyme in eukaryotes is ex-

pressed as isozymes, two in yeast (called 1 and 2) and three in vertebrates, called α , β and γ . Enolase α is ubiquitous, found in all cells. Enolase β is muscle-specific and the γ isozyme is found only in neurons. These enzymes, as isolated, are mixtures of hetero- and homodimers. We are concerned with whether or not the subunits catalyze their reaction independently or whether some catalytically significant interaction between enolase subunits occurs.

2. Materials and methods

Human neuronal enolase (with a his-tag) was expressed in *E. coli* and isolated as described [8]. Specific activities were consistent with those reported for samples of enzyme that were crystallized ($130 \pm 10 \Delta OD_{230}/\text{minute}/\Delta OD_{280}$). After correction [9] for the effects of pH (6.9) and KCl concentration (0.4 M), k_{cat} is about 45 s^{-1} . For calculations of concentration, an extinction coefficient, obtained using the residue absorbencies of Perkins [10] of 0.87/mg/ml and a subunit molecular weight of 48 015 were employed.

Yeast enolase 1 was also obtained as described [11]. Its specific activity was also consistent with previously reported values [12]: a k_{cat} of ca. 125 s^{-1} . Enzyme assays were performed at ambient room temperature, which varied from 21° to 24° .

The final purification step of the enzymes is carried out in a tris (tris (hydroxymethyl) aminomethane) buffer. For stopped-flow

Abbreviations: TSP, D-tartronate semialdehyde phosphate; 2-PGA, 2-phospho-D-glycerate; PEP, phosphoenolpyruvate; PIPES, piperazine-N,N'-bis(2-ethane sulfonic acid); HEPES, hydroxyethylpiperazine-N'-2-ethane sulfonic acid; tris, tris (hydroxymethyl) aminomethane

* Corresponding author. Fax: +1 706 542 1738.

E-mail address: brewer@bmb.uga.edu (J.M. Brewer).

reactions in piperazine-*N,N*-bis(2-ethane sulfonic acid) (PIPES) or hydroxyethylpiperazine-*N'*-2-ethane sulfonic acid (HEPES), the pooled fractions were concentrated by pervaporation, precipitated with 75% ammonium sulfate, then the precipitate was dissolved and dialyzed over 24–48 h against three changes of PIPES or HEPES.

Stopped-flow measurements were done using the RSM-1000 (rapid-scanning module) from Olis, Inc. (Bogart, GA) at ambient room temperature (about 22°).

Reagents were AR grade; 2-PGA was from Sigma–Aldrich (St. Louis, MO) as were HEPES and PIPES. Tris was from BioRad. TSP was synthesized as described by Spring and Wold [13]. The very strongly bound competitive inhibitor phosphono-acetohydroxamate was prepared and assayed as described by Anderson et al. [14].

3. Results

We carried out steady-state activity measurements to delineate the effects of various parameters on the physiological reaction (2-PGA → PEP) catalyzed by the human neuronal enolase. Some preliminary enzymatic characteristics have been reported [8,15]. Activation constants for Mg^{2+} and K_m values for 2-PGA which we measured were in good agreement.

The effect of pH on the V_{max} of the human neuronal enolase was determined, varying the Mg^{2+} concentration at each pH value. An optimum pH (corrected) [9] of 7.2–7.4 was observed (not shown), and we used buffers at pH 7.2 and 7.5 for the stopped-flow measurements. The human neuronal enzyme, like yeast enolase 1, is inhibited by Mg^{2+} concentrations above 1 mM [16] (also not shown). Yeast enolase 1 has a pH optimum of 7.7 [17] and we employed HEPES–NaOH at pH 7.6 and tris–HCl at pH 7.8 for stopped-flow measurements with that enzyme.

Originally, we wished to see if Mg^{2+} concentrations above 1 mM inhibited the TSP reaction; in other words, is the inhibition of the physiological reaction due to slowing product (PEP) release [5,18], or, a possibility suggested by Faller et al. [2], due to binding of a third, inhibitory Mg^{2+} at the active site?

The TSP reaction requires catalytic Mg^{2+} binding [19] and can be monitored using stopped-flow measurements [20]. This is a measurement of a single turnover, since the TSP enolate picks up a proton and isomerizes to the non-absorbing (over 250–320 nm) keto form when it dissociates [4,6]. The OLIS RSM apparatus measures the absorption spectrum of two solutions mixed rapidly (in ca. 2 ms), at 1 ms intervals thereafter. We routinely used 18–20 μ M enzyme, and the OLIS cuvette has an optical pathlength of 1 cm, so we were measuring maximum absorbencies around 280 nm of about 0.5–0.6.

We present results of measurements made at three Mg^{2+} concentrations, 100 μ M, 1 mM and 30 mM, which for the physiological (2-PGA → PEP) reaction are below saturation, saturating and inhibitory, respectively [2,16]. Both the human neuronal enolase and yeast enolase 1 interact with tris [8,21], so we used that buffer and also two “non-interacting” buffers, PIPES and HEPES, for comparison. Global fits were made to data collected over the wavelength range 250–320 nm. The data were fitted to various kinetic schemes until a satisfactory fit, judged from the randomness of the absorbance residuals as functions of time after mixing, was seen.

The reactions of several preparations of the human and yeast enzymes and of TSP gave consistent results: all reactions could be fit only by assuming biphasic (each first order) kinetics (Fig. 1). The data are equally well fit assuming two successive reactions or two parallel ones. The data presented in Fig. 1 are representative examples showing effects of low and high magnesium ion concentrations and some different fitting models. We present

the kinetic and absorbance parameters from the simplest kinetic scheme giving satisfactory fits in Table 1. All parameters are means and standard deviations of three or four replicate measurements. We also find that higher Mg^{2+} concentrations reduced the apparent extent (ΔOD) of the slower reaction in absolute terms, while increasing that of the faster.

The “30 mM” data shown in Table 1 involve mixing enolase solutions containing 0.1 mM Mg^{2+} with 60 mM Mg^{2+} plus TSP solution, so there is a significant increase in ionic strength. We also performed stopped-flow measurements in which yeast enolase 1 with 30 mM Mg^{2+} present was mixed with 30 mM Mg^{2+} plus TSP. Also, we carried out those measurements using solutions that also contained 0.15 M KCl, as this produces a small (15–20%) increase in the rate of the physiological reaction (unpublished observations). In addition, we carried out stopped-flow measurements in which the yeast enzyme in 30 mM Mg^{2+} containing subsaturating levels (0.25 and 0.5 moles per mole of active site) of TSP or the very strongly bound competitive inhibitor phosphono-acetohydroxamate [14] were mixed with 30 mM Mg^{2+} plus TSP (not shown). In no case did we observe single first-order kinetics; all data were fit, assuming either two successive first order or two parallel first-order reactions and the rates obtained were consistent with those presented in Table 1.

The software supplied with the OLIS RSM enables us to reconstruct the absorption spectra of all assumed fitted species. These are of varying magnitudes, depending on the Mg^{2+} concentration, but may be normalized to a common maximum magnitude for the sake of comparison.

These calculated difference spectra were obtained using the human neuronal enolase in tris and in PIPES. They were very similar but the spectra obtained at 100 μ M Mg^{2+} corresponding to the slower reaction were shifted 2–3 nm to longer wavelengths relative to those of the faster (not shown). At 30 mM Mg^{2+} , the spectra are closer but those of the faster reaction are perhaps at 1 nm shorter wavelengths. This suggests the Mg^{2+} concentration affects the environments of the TSP enolates, but does not permit us to distinguish between alternative kinetic models.

The two successive reaction kinetic model is applicable only if the first step is controlled – produced – by catalytic Mg^{2+} binding. Hence, suppression of a second consecutive slower reaction by higher Mg^{2+} concentrations makes no sense, since a slower second consecutive reaction must be rate limiting. We conclude two parallel reactions is the more likely mechanism.

There is considerable crystallographic evidence [8,22–24] that binding of substrate/analogues at the active sites of both enzymes is accompanied by movement of polypeptide loops that close around the active sites. (Since crystals are routinely prepared with saturating levels of all ligands, it is not presently possible to say whether substrate binding alone – no catalytic Mg^{2+} bound – produces any loop(s) movement, but it is plausible that some movement occurs [7].) This movement is transmitted between the subunits, producing binding of 2-PGA in one subunit and PEP in the other [24, L. Lebioda, personal communication]. Since the TSP enolization kinetics are always complex, we interpret our data in terms of subunit interactions involving catalysis.

At low Mg^{2+} concentrations (50 or 100 μ M) but high TSP concentrations (100 or 200 μ M), some enolase molecules will have TSP bound in both subunits but catalytic Mg^{2+} in only one. Our results suggest the subunit with bound TSP but no catalytic Mg^{2+} shows the TSP reaction in the other subunit, so that the slower reaction contributes a larger fraction of the total absorbance change. This is consistently observed (Table 1).

The increases in rate of the faster reaction produced by higher Mg^{2+} concentrations in PIPES or HEPES buffers could be interpreted in terms of an anticooperative binding of catalytic Mg^{2+} . Stopped-flow measurements of TSP enolization rates at

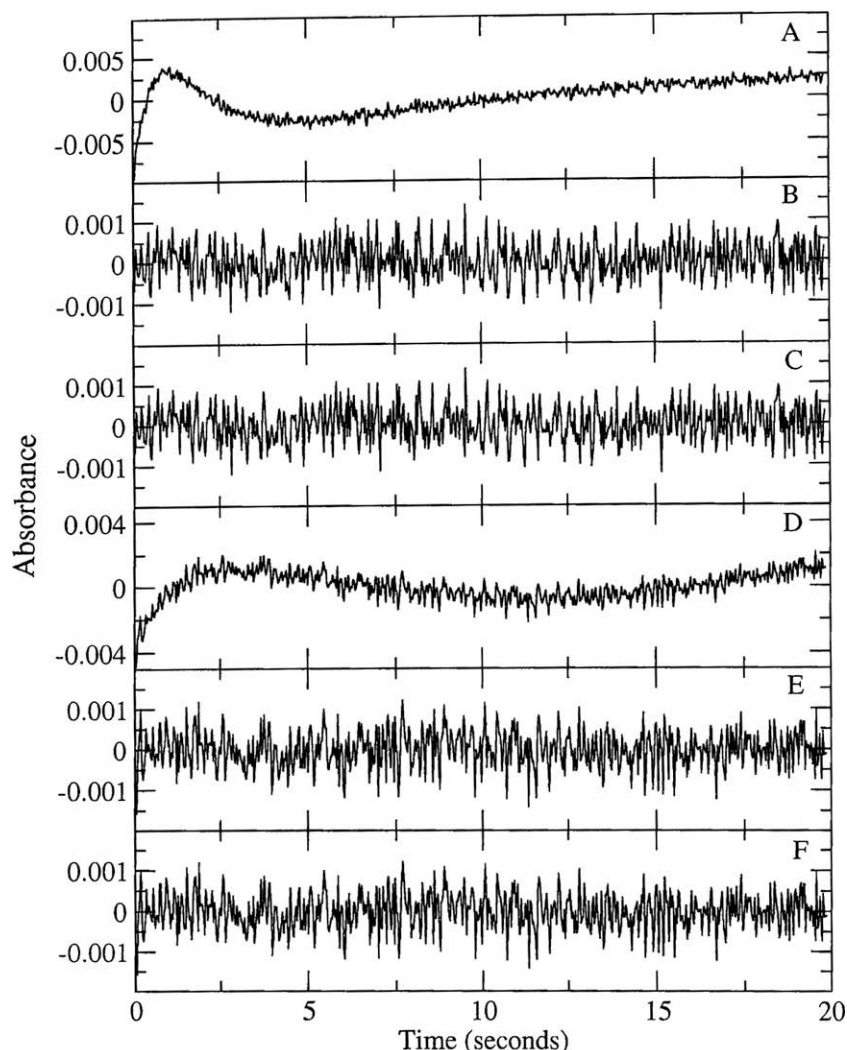


Fig. 1. Examples of residuals plots of attempted fits to the stopped-flow data from two reactions, assuming (A and D) a single first-order reaction; (B and E) two successive first-order reactions; (C and F) two independent (parallel) first-order reactions. The upper reaction (A, B and C) was of yeast enolase 1 (10 μM subunits after dilution) reacting with 200 μM (after dilution) TSP with 30 mM Mg^{2+} (after dilution), present. The lower reaction (D, E and F) had 50 μM Mg^{2+} (after dilution) present. Both of these particular reactions were performed in 0.05 ionic strength tris-HCl, pH 7.8.

other Mg^{2+} concentrations, 4 and 20 mM with yeast enolase 1, and 3 and 10 mM with the human enzyme (not shown) are consistent with this interpretation. Evidence from steady-state kinetics of the physiological reaction (2-PGA \rightarrow PEP) obtained using four yeast enolase mutants (H159N, A, F and N207A), all with changes in a residue involved in loop movement or one participating in intersubunit interaction, suggest this [12]. However, another explanation is possible for the higher rates observed at 30 mM Mg^{2+} . Higher Mg^{2+} concentrations promote increased average closure of loops around the active sites. This dynamic process produces a population of enolase molecules, some with one subunit without catalytic Mg^{2+} bound that slows the TSP reaction in the others subunit. So the contribution of the slower reaction to the total is reduced but not eliminated at 30 mM Mg^{2+} . A higher Mg^{2+} concentration stabilizes the closed and more reactive subunit conformation simply by mass action.

(The inhibition of the rate of reaction of the physiological substrate by Mg^{2+} concentrations above 1 mM occurs because the stabilized closure of the peptide loops about the active site reduces the rate of product release [16].)

Beyond that, the effects observed of Mg^{2+} concentration in tris buffers are difficult to rationalize. A molecule of tris binds to the

subunit of human neuronal enolase that also binds a sulfate at the active site [8]. There may be a synergistic relation between TSP and tris binding at one subunit, but this is speculative.

The data also show seemingly erratic, though often significantly different, rates of the slower reaction at the different Mg^{2+} concentrations. Further analyses, crystallographic as well as kinetic, may clarify these points.

4. Discussion

Lane and Hurst [20] carried out stopped-flow-temperature jump analyses in 1 mM Mg^{2+} of the reaction of TSP and other analogues with yeast enolase 1. No buffer was employed. At 4°, the reactions with TSP appeared to be first order, though detailed analysis of the kinetics on the basis of oscilloscope tracings was not feasible. Our results show how dramatically both instrumentation and software have improved in the 30 years since then. They also concluded that TSP bound rapidly but reacted more slowly. Thus, a certain amount of time in which catalytic Mg^{2+} remains bound to the enzyme-TSP complex is necessary to produce proton loss and enolization of the TSP. This time would be within the dead time of the stopped-flow, as no lag phase has been observed by them or by us.

Table 1

Kinetic parameters obtained from reaction of human neuronal enolase and yeast enolase 1 with TSP.

Buffer	[Mg ²⁺] _{final}	[TSP] _{final}	<i>k</i> ₁ (s ^{−1})	<i>k</i> ₂ (s ^{−1})	Δ <i>A</i> ₁ (ΔOD ₂₈₅)	Δ <i>A</i> ₂ (ΔOD ₂₈₅)
A. Yeast enolase						
0.05 M HEPES–NaOH, pH 7.6	50 μM	100 μM	1.31 ± 0.14	0.278 ± 0.004	0.042 ± 0.001	0.070 ± 0.003
	100 μM	100 μM	1.08 ± 0.11	0.339 ± 0.014	0.060 ± 0.0003	0.062 ± 0.002
	100 μM	200 μM	0.81 ± 0.03	0.308 ± 0.004	0.096 ± 0.002	0.035 ± 0.002
	1 mM	100 μM	1.02 ± 0.04	0.024 ± 0.008	0.145 ± 0.001	0.013 ± 0.004
	30 mM	100 μM	2.94 ± 0.03	0.41 ± 0.08	0.145 ± 0.002	0.005 ± 0.0001
	30 mM	200 μM	3.14 ± 0.09	0.525 ± 0.25	0.141 ± 0.003	0.008 ± 0.002
<i>I</i> /2 = 0.05 tris–HCl, pH 7.8	50 μM	100 μM	0.45 ± 0.04	0.060 ± 0.003	0.019 ± 0.008	0.036 ± 0.003
	50 μM	200 μM	0.46 ± 0.04	0.062 ± 0.004	0.017 ± 0.0007	0.040 ± 0.0002
	100 μM	100 μM	0.61 ± 0.16	0.071 ± 0.006	0.015 ± 0.0013	0.050 ± 0.002
	1 mM	100 μM	0.75 ± 0.05	0.244 ± 0.027	0.062 ± 0.006	0.079 ± 0.006
	30 mM	100 μM	0.92 ± 0.061	0.216 ± 0.047	0.143 ± 0.004	0.011 ± 0.005
	30 mM	200 μM	1.15 ± 0.026	0.087 ± 0.011	0.154 ± 0.0004	0.007 ± 0.001
B. Human neuronal enolase						
					Δ <i>A</i> ₁ (ΔOD ₂₉₁)	Δ <i>A</i> ₂ (ΔOD ₂₉₁)
0.05 M PIPES–NaOH, pH 7.2	100 μM	100 μM	6.4 ± 1.1	1.3 ± 0.5	0.012 ± 0.010	0.059 ± 0.009
	1 mM	100 μM	7.7 ± 0.6	1.24 ± 0.4	0.060 ± 0.006	0.036 ± 0.004
	30 mM	100 μM	13.5 ± 3.8	3.0 ± 2.2	0.050 ± 0.035	0.042 ± 0.017
<i>I</i> /2 = 0.05 tris–HCl, pH 7.5	100 μM	100 μM	14.1 ± 2.0	3.0 ± 0.2	0.041 ± 0.008	0.045 ± 0.005
	1 mM	100 μM	20.1 ± 3.4	7.09 ± 0.8	0.042 ± 0.044	0.052 ± 0.014
	30 mM	100 μM	17.0 ± 1.3	4.5 ± 0.8	0.095 ± 0.009	0.019 ± 0.006

Kinetic parameters obtained upon reaction of TSP with enolases in the stopped-flow apparatus. The enzymes (18.5 or 20 μM subunits) in the buffers shown were mixed with equal volumes of the same buffer containing *D*-TSP; sufficient Mg²⁺ was present in the TSP solutions to produce the final concentrations indicated. The parameters were obtained, assuming two parallel reactions were occurring: A → B, C → B, and are averages and standard deviations obtained between 250 and 320 nm and 3 or 4 replicate measurements.

Our data show no inhibition of the TSP reaction at Mg²⁺ concentrations (30 mM) that are inhibitory to the steady-state physiological reaction, that is, there is no evidence for binding of inhibitory Mg²⁺, consistent with the interpretation of Poyner et al. [18].

X-ray crystallographic studies of the human neuronal enolase complexed with substrate/product show no evidence of a third equivalent of Mg²⁺ bound at the active sites even at free Mg²⁺ concentrations of 200 mM (L. Lebiada, personal communication).

Otherwise, the salient finding is that with both enolases, under all conditions (buffer, pH, Mg²⁺ and TSP concentrations) employed by us, the kinetics are biphasic: fits using a single exponential are not satisfactory. If the subunits reacted independently, we would not see this.

The next most obvious result is that higher concentrations of Mg²⁺ or, to some extent higher TSP concentrations, reduce the amplitude of the slower phase. Since substrate and Mg²⁺ binding are ordered and interdependent [5,18] that is equivalent to saying that more extensive or complete saturation by catalytic Mg²⁺ binding produces the effect.

The observed effect of Mg²⁺ indicates that optical or electronic artifacts are not a factor. It also indicates that a secondary relaxation of the initial product of TSP enolization is not the cause of the kinetics observed; the slower reaction is not obligatory, in other words. The observation with the human enzyme that the product of the slower reaction has an absorption spectrum significantly shifted, relative to the product of the faster one, could also be explained by a difference in environment of the TSP in the two subunits. The crystallographic structure of human neuronal enolase complexed with TSP shows a marked difference in the TSP bound in the two subunits (L. Lebiada, personal communication), though the time scale over which this difference develops is uncertain.

There is a minor controversy over whether enolase subunits catalyze their reactions independently or whether there is some interaction between subunits that affects their turnover. It has been shown that yeast enolase 1 subunits dissociated in the presence of Mg²⁺ have some level of activity [25]. The X-ray crystallographic data show intersubunit interactions occurring through N207 in yeast enolase 1 [11]. The N207A mutant of that enzyme has 22% of the activity of native enolase at 1 mM Mg²⁺, but also

shows a biphasic Mg²⁺ activation, so the maximum activity of N207A enolase, extrapolated to infinite Mg²⁺ concentration, is 56% of native yeast enolase 1 [12], the latter assayed at 1 mM Mg²⁺, the normal optimal concentration.

Sims et al. [23] prepared a heterodimer of yeast enolase 1 (with two surface residues modified to make chromatographic separation easier) and the K345A mutant, and obtained the crystal structure with bound substrate. The *k*_{cat} value of the heterodimer was 35–50% of the homodimer of wild type enolase, depending on what reference is employed. These authors also suggested the asymmetry between yeast enolase subunits is an artifact of the crystal packing.

However, the his-tagged human neuronal enolase crystallizes in a different space group and also exhibits asymmetry between subunits [8]. The data presented here use unmutated (except for the his-tag) enzymes and are not consistent with independently catalyzing subunits. They are easily consistent with catalytically significant interaction. We suggest a reduction of turnover (*k*_{cat}) owing to the association of enolase subunits to about 60 ± 20% occurs. This is reasonably consistent with all these observations. Because of the abundant expression of enolases, this would have no physiological significance, but results from the generally cooperative nature of interactions producing the levels of protein structure. Nor should this be surprising: movement of polypeptide chains during catalysis of multisubunit enzymes is often transmitted between subunits and may affect activity; indeed, complete enzymatic independence of subunits would seem anomalous.

References

- [1] Brewer, J.M. (1981) Yeast enolase: mechanism of activation by metal ions. *CRC Crit. Rev. Biochem.* 11, 209–254.
- [2] Faller, L.D., Baroudy, B.M., Johnson, A.M. and Ewall, R.X. (1977) Magnesium ion requirements for yeast enolase activity. *Biochemistry* 16, 3864–3869.
- [3] Westhead, E.W. (1966) Enolase from yeast and rabbit muscle. *Methods Enzymol.* 9, 670–679.
- [4] Spring, T.G. and Wold, F. (1971) Studies on two high-affinity enolase inhibitors. Reaction with enolases. *Biochemistry* 10, 4655–4660.
- [5] Shen, T.Y.S. and Westhead, E.W. (1973) Divalent cation and pH-dependent primary isotope effects in the enolase reaction. *Biochemistry* 12, 3333–3337.

- [6] Weiss, P.M., Boerner, R.J. and Cleland, W.W. (1987) The catalytic base of enolase is a sulfhydryl group. *J. Am. Chem. Soc.* 109, 7201–7202.
- [7] Brewer, J.M. and Lebiada, L. (1997) Current perspectives on the mechanism of catalysis by the enzyme enolase. *Adv. Biophys. Chem.* 6, 111–141.
- [8] Chai, G., Brewer, J.M., Lovelace, L.L., Aoki, T., Minor, W. and Lebiada, L. (2004) Expression, purification and the 1.8 Å resolution crystal structure of human neuron specific enolase. *J. Mol. Biol.* 341, 1015–1021.
- [9] Wold, F. and Ballou, C.E. (1957) Studies on the enzyme enolase. I. Equilibrium studies. *J. Biol. Chem.* 227, 301–312.
- [10] Perkins, S.J. (1986) Protein volumes and hydration effects. *Eur. J. Biochem.* 157, 169–180.
- [11] Brewer, J.M., Glover, C.V.C., Holland, M.J. and Lebiada, L. (1998) Significance of the enzymatic properties of yeast S39A enolase to the catalytic mechanism. *Biochim. Biophys. Acta* 1383, 351–355.
- [12] Brewer, J.M., Glover, C.V.C., Holland, M.J. and Lebiada, L. (2003) Enzymatic function of loop movement in enolase: preparation and some properties of H159N, H159A, H159F and N207A enolases. *J. Prot. Chem.* 22, 353–361.
- [13] Spring, T.G. and Wold, F. (1971) Studies on two high-affinity enolase inhibitors. Chemical characterization. *Biochemistry* 10, 4649–4654.
- [14] Anderson, V.E., Weiss, P.M. and Cleland, W.W. (1984) Reaction intermediate analogues for enolase. *Biochemistry* 23, 2779–2786.
- [15] Marangos, P.J. and Schmechel, D.E. (1987) Neuron specific enolase, a clinically useful marker for neurons and neuroendocrine cells. *Annu. Rev. Neurosci.* 10, 269–295.
- [16] Wold, F. and Ballou, C.E. (1957) Studies on the enzyme enolase. II. Kinetic studies. *J. Biol. Chem.* 227, 313–328.
- [17] Wold, F. (1971) Enolase in: *The Enzymes* (Boyer, P.D., Ed.), third ed, pp. 499–538, Academic Press, NY.
- [18] Poyner, R.R., Cleland, W.W. and Reed, G.H. (2001) Role of metal ions in catalysis by enolase: an ordered kinetic mechanism for a single substrate enzyme. *Biochemistry* 40, 8009–8017.
- [19] Spencer, S.G. and Brewer, J.M. (1984) Activation of yeast enolase by Cd(II). *J. Inorg. Biochem.* 20, 39–52.
- [20] Lane, R.H. and Hurst, J.K. (1974) Intermediates in enolase-catalyzed reactions. *Biochemistry* 13, 3292–3297.
- [21] Brewer, J.M., Faini, G.J., Wu, C.A., Goss, L.P., Carreira, L.A. and Wojcik, R. (1978) Characterization of the subunit dissociation of yeast enolase in: *Physical Aspects of Protein Interactions* (Catsimopoulos, N., Ed.), pp. 57–78, Elsevier-North Holland, New York.
- [22] Qin, J., Chai, G.C., Brewer, J.M., Lovelace, L.L. and Lebiada, L. (2006) Fluoride inhibition of enolase: crystal structure and thermodynamics. *Biochemistry* 45, 793–800.
- [23] Sims, P.A., Menefee, A.L., Larsen, T.M., Mansoorabadi, S.O. and Reed, G.H. (2006) Structure and catalytic properties of an engineered heterodimer of enolase composed of one active and one inactive subunit. *J. Mol. Biol.* 355, 422–431.
- [24] Zhang, E., Brewer, J.M., Minor, W., Carreira, L.A. and Lebiada, L. (1997) Mechanism of enolase: the crystal structure of asymmetric dimer enolase-2-phospho-D-glycerate/enolase-phosphoenolpyruvate at 2.0 Å resolution. *Biochemistry* 36, 12526–12534.
- [25] Holleman, W.H. (1973) The use of absorption optics to measure dissociation of yeast enolase into enzymatically active monomers. *Biochim. Biophys. Acta* 327, 176–185.